Research Article | Vol. 27, No. 25 / 9 December 2019 / Optics Express 36741
Optics EXPRESS

Compact, high repetition rate, 4.2 MW peak power, 1925 nm, thulium-doped fiber chirped-pulse amplification system with dissipative soliton seed laser

ZHENGQI REN,* QIANG FU, LIN XU, JONATHAN H. V. PRICE, SHAIF-UL ALAM, AND DAVID J. RICHARDSON

Optoelectronics Research Centre, University of Southampton, Southampton SO17 1BJ, UK
*zr2y14@soton.ac.uk

Abstract: We report the demonstration of a high average- and peak-power, 1925 nm, thulium-fiber based chirped pulse amplification (CPA) system. A compact, dissipative soliton thulium-fiber, mode-locked seed produced pre-chirped pulses with 25 ps duration, 45 mW output power and repetition rate of 15.7 MHz. After stretching to 105 ps in 83 m of normal dispersion fiber, the pulses were amplified in a core-pumped pre-amplifier and a cladding pumped power amplifier to average output powers of 28 W and 30 W with forward and backward pumping, respectively, with the output power limited only by the available pump power. After a pair of fused silica transmission gratings with an efficiency of 71%, the amplified pulses were re-compressed to 297 fs yielding pulses with a peak power of 4.2 MW (backward pumped) and a pulse energy of 1.27 μJ.

1. Introduction

High power and high energy ultra-short-pulse fiber lasers at 2 μm are attractive for many applications including free space optical communications, sensing, material processing and mid-IR generation [1–4]. High energy applications in the 2 μm range in particular, such as high harmonic generation [5] and laser-driven electrons acceleration [6], would benefit from repetition-rate scaling. While ultimately this may be realized using rod-type and/or coherently combined fiber amplifiers in the future [7–9], here we focus on developing systems with more conventional, flexible, fiber technology which is an important research target with immediate practical applications including material processing and mid-IR light generation.

Recent demonstrations of 2 μm thulium-doped fiber laser systems based on chirped pulse amplification (CPA) have enabled fs pulse generation with μJ energies [7,10,11]. For example, 1 μJ energy and 3 MW peak power in 300 fs pulses was demonstrated by Sims *et al.* using a conventional large-mode-area fiber [10]. Later, pulses with both higher 4 MW peak power and 152 W average power were realized through the use of thulium doped photonic crystal fiber (PCF) with 50 μm core diameter and by stretching the seed pulse much more than others to a duration of 400 ps [7]. The highest recorded average power (1 kW/50 MW peak), used the same PCF as discussed above and further increased the stretched pulse duration to 1 ns using two customized chirped volume Bragg gratings (CFBG) [12]. The use of rods compromises on compactness/generally requires free space signal coupling and we would suggest that this is perhaps not ideal for many industrial settings. After that, by using a chirped volume Bragg grating (CVBG) as a temporal stretcher and compressor, Hoogland *et al.* realized pulses with 1 MW peak power at 371 fs duration based on conventional large mode area fiber [11]. However,

#375939 https://doi.org/10.1364/OE.27.036741
Journal © 2019 Received 21 Aug 2019; revised 31 Oct 2019; accepted 4 Nov 2019; published 4 Dec 2019

Optics EXPRESS

the use of bulk or free space optical elements to stretch the pulses rather than monolithically integrated pulse stretchers compromises the long-term stability [7,11]. Furthermore, systems [10,11] which use pulse-pickers to increase the pulse energy have unwanted insertion losses requiring the addition of more amplification stages. In order to improve stability, systems with an all-fiber pulse pre-stretcher have been demonstrated. In one case, the output of the oscillator was stretched in a 50 m long normal dispersion fiber and then amplified in a two stage MOPA to produce 161 nJ pulses after a grating pair compressor [13]. However, there, the relatively small mode area of the gain fiber limited further energy scaling due to self-phase-modulation (SPM). To keep the dispersion elements compact, pulses have been stretched in a CFBG and subsequently re-compressed with a CVBG, but then a pulse-picker reduced the repetition rate to 92 kHz limiting the average power to just 0.64 W (4 μJ pulse energy, 2.4 MW peak power) [14].

Here, we present a compact and simple dissipative soliton seeded thulium-fiber CPA system outputting high peak and average powers at 1925 nm. A normal-dispersion fiber based pulse stretcher, use of just two amplification stages, and a high-efficiency transmission grating compressor, enabled excellent performance to be achieved with a highly practical and compact system when compared to those reported previously. Via careful optimisation of the seed laser and fiber amplifiers, the final system generated 1.25 μJ energy, 297 fs pulses with 4.2 MW peak power, 21.5 W average power and beam quality M^2 of 1.1 at a repetition rate of 15.7 MHz. The output was pump-power limited and options for power scaling are therefore discussed.

2. Experimental setup

The system schematic is shown in Fig. 1. The upper section shows the mode-locked, uni-directional ring laser seed incorporating a homemade 1560 nm erbium-doped fiber pump laser (EDFL) coupled to 2 meters of single-mode thulium-doped fiber (TDF) (OFS, TmDF200) with a 1560/1960 nm wavelength-division multiplexer (WDM). The TDF has ~20 dB/m absorption at 1560 nm and a group velocity dispersion of approximately -0.02 ps^2/m at 1.9 μm. A compact in-line polarization controller (PC) (FIBERPRO PC1100) with 0.2 dB insertion loss and semiconductor saturable absorber mirror (SESAM) (Batop). We estimate that the nonlinear pulse propagation in the NDF and TDF inside the cavity during mode-locked operation gives rise to a total B-integral of ~0.8π, and the cavity circulator provides a polarization dependent loss of 0.6 dB as required to sustain nonlinear polarization rotation (NPR). Hence, as is common for dissipative soliton lasers, we used the SESAM to initiate self-starting and NPR to stabilize the pulses by appropriate adjustment of the intracavity polarization controller. The 70% port of a tap coupler was used to extract the output for subsequent amplification. A 5.2 m section of normal dispersion fiber (NDF) (Nufern Inc. UHNA4; 0.09 ps^2/m at 1900 nm) was placed between the circulator and the WDM for dispersion management [15,16]. The fiber pigtails of all the components were of Corning SMF 28 (dispersion -0.067 ps^2/m at 1900 nm). Considering the total SMF length of 6 m and the total cavity length of 13.2 m we estimate the net dispersion of the cavity to be ~0.026 ps^2.

For the stretcher, 58 m NDF (Nufern Inc. UHNA7) (with dispersion of 0.046 ps^2/m) and 25 m of UHNA4 provided total dispersion of 4.9 ps^2. The combination of UHNA4 and UHNA7 enabled better compression results than a single fiber type due to their opposite sign of third order dispersion [16]. The pre-amplifier comprised a 1 m length of 5/125 μm core/cladding diameter TDF from OFS (TmDF200), backward pumped by a 1560 nm EDFL. A non-PM pre-amplifier was used due to short term component availability, this would ideally be upgraded in due course to provide a fully PM system - however this did not compromise the current experiments. A second PC is incorporated after the pre-amplifier to orient the polarization of the pulses to the transmission axis of the PM isolator, generating pulses with linear polarization to obtain optimum transmission ratio through the compression gratings.

Optics EXPRESS

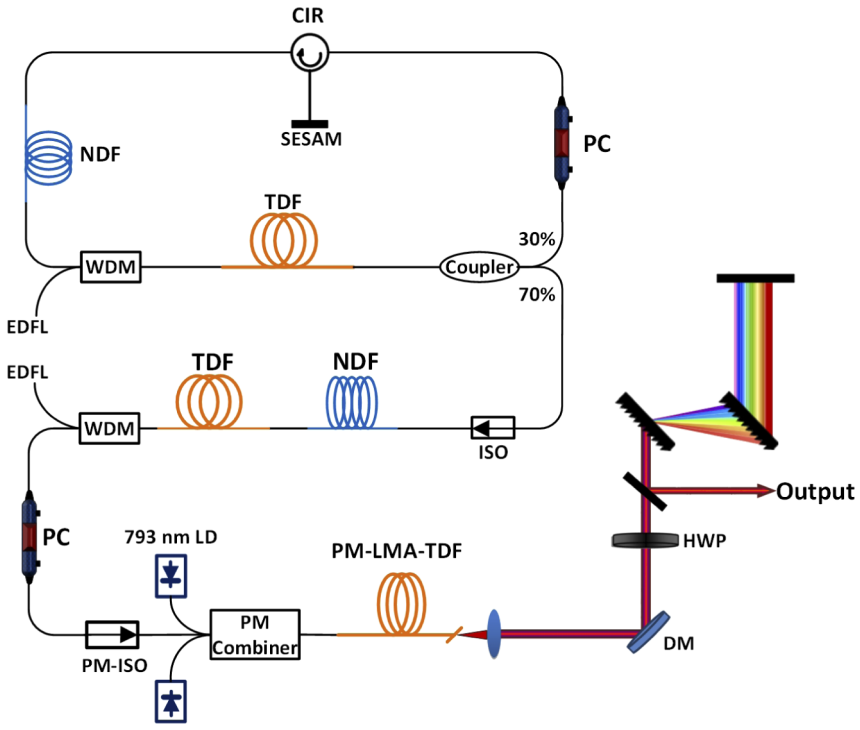

Fig. 1. Schematic of the CPA system. WDM-Wavelength-division multiplexer, PC-Polarization controller, CIR- Circulator, DM- Dichroic mirror.

For the final amplifier, we first tested a fully fiberized forward pumping configuration with resultant advantages in terms of long-term stability, as shown in Fig. 1. We then tested a free-space reverse-pumped amplifier which both reduced the effective nonlinear length [17,18] and, as a bonus, shifted the gain peak to more closely align with that of the seed pulse spectrum. The power amplifier comprised a 1.5 m length of PM double-clad (DC) TDF with a 25 μm core diameter (largest core size available commercially). As detailed below the short fiber length and large core area enabled energy scaling without excessive nonlinearity. The fiber was forward pumped by fiber-pigtailed 793 nm multimode diodes (BWT) via a $(6 + 1) \times 1$ polarization maintaining (PM) pump combiner (LightComm), or reverse pumped but still using the same 793 nm diodes. An angle polished (8°) 1 mm long, 400 μm diameter, endcap was spliced to the output end of the TDF to the Fresnel reflection from the glass-air interface and the fiber was mounted on a water-cooled plate using graphite tape to ensure good thermal transfer. The amplified pulses were collimated by a calcium fluoride lens (f = 15 mm) and compressed by a pair of fused silica transmission gratings (Ibsen Photonics A/S) with 560 lines/mm and single pass transmission efficiency 94% across the 1900-2100 nm wavelength range. The width of the grating governs the maximum delay between short and long wavelength components, and for our pulses with 40 nm spectral bandwidth the 25 mm wide transmission grating can provide maximum -6.4 ps^2 of dispersion in our double pass setup. A 12.5 GHz InGaAs photodetector (EOT ET-5000F) with a 200 MHz oscilloscope (Agilent DSO-X 2024A) and an electrical spectrum analyzer (Agilent E4446A) were used to measure the pulse characteristics in the electrical domain. The pulse duration was measured with a non-collinear SHG autocorrelator (APE Pulse-check) and the pulse spectra were measured using an optical spectrum analyzer (Yokogawa AQ6375).

Optics EXPRESS

3. Experimental results and analysis

With appropriate adjustment of the polarization controllers in the laser cavity (Fig. 1), self-starting and stable mode-locked operation was achieved at a pump power of 400 mW (used for all the CPA results shown below). The corresponding output power was 40 mW and the pulse energy was 2.5 nJ. The laser would maintain stable operation and provided increased output power of 45 mW when the pump power was increased to 420 mW, but both the pulse train on the oscilloscope and the optical spectra became unstable at higher pump powers. The measured repetition rate of 15.7 MHz shown in Fig. 2(a) was in agreement with calculations based on the cavity length, supporting our conjecture that the oscillator operates with a single pulse per round trip. The insert in Fig. 2(a) shows the measured autocorrelation of the positively chirped output with an inferred pulse width of 25 ps (assuming a Gaussian pulse shape). The radio-frequency (RF) spectrum (Fig. 2(b)) exhibits a ~71 dB signal-to-noise ratio measured with a range of 10 kHz and a resolution bandwidth of 10 Hz, indicating the stability of the mode-locking. We attribute the small peaks offset by 23 kHz from the fundamental cavity frequency to be due to relaxation oscillations [19,20]. The RF spectrum with a frequency span of 1 GHz is shown inset to Fig. 2(b) with resolution bandwidth of 1 MHz.

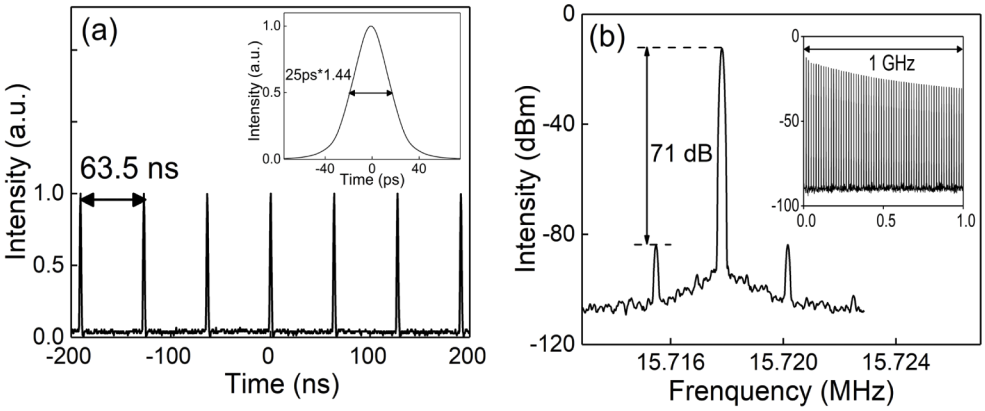

Fig. 2. (a) Oscilloscope trace of the output pulses. Inset: autocorrelation trace of the seed laser. (b) RF spectrum at the fundamental frequency of 15.7 MHz. Inset: RF spectrum with 1 GHz span.

We were able to achieve a limited degree of spectral amplitude shaping from the oscillator output through precise adjustment of the PC. This was used to pre-compensate the low gain at shorter wavelengths in the intentionally under-length power amplifier. The oscillator spectrum used for the forward pumped amplifier configuration, measured with a resolution of 0.05 nm, is shown in Fig. 3 (black line). The center wavelength was 1925 nm, the 10 dB width was ~40 nm and the shape had the characteristic steep spectral edges associated with dissipative soliton mode-locking [21]. The signal was 27 dB above the ASE floor.

To reduce the nonlinear phase shift in the 83 m long stretcher fiber the power was decreased to 4 mW with an attenuator at the stretcher input. The stretched pulses were measured to have a deconvolved duration of 105 ps and were amplified to an average power of 180 mW in the pre-amplifier. This power was chosen to avoid unnecessary non-linear phase yet to still have sufficient signal power to saturate the subsequent power amplifier. After adjustment of the PC before the the fast-axis blocking isolator between the pre- and power-amplifier the spectrum was as shown in Fig. 3 (blue line). The average power at the input of the final amplifier reduced to 120 mW because some degree of depolarization in the long length of non-PM stretcher fiber led to an excessive the isolator insertion loss. The slope on the pre-amplifier spectrum was then

Optics EXPRESS

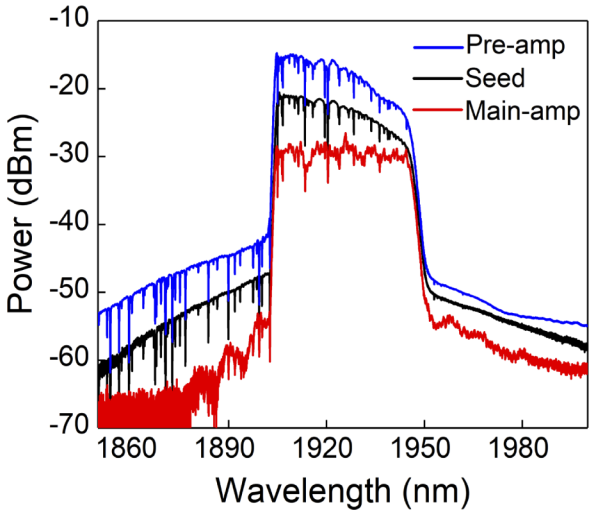

Fig. 3. The optical spectrum of the seed laser (black) and the pre-amplified (blue), main amplified pulses (red) at the maximum output power obtained with the forward pumped version of the power amplifier.

compensated by the gain of the power amplification stage, giving the flat compressed output spectrum shown by the red line in Fig. 3. The peak voltage vs. the voltage of the background signal between pulses measured directly from the oscillator, pre-amplifier and the power amplifier using a 12.5 GHz photodetector (EOT ET-5000F) and our 1 GHz bandwidth analog oscilloscope (Tektronix 7104) was always greater than 28 dB (measurement limited by the dynamic range of the oscilloscope and detector dark current). With forward pumping, the power amplifier boosted the power to 28 W (17 kW peak power) using the full 104 W of available pump. The slope efficiency was 28% with respect to coupled pump power, as shown in Fig. 4(a). The residual pump at the fiber output when operating at the maximum power in this forward pump configuration was 13 W.

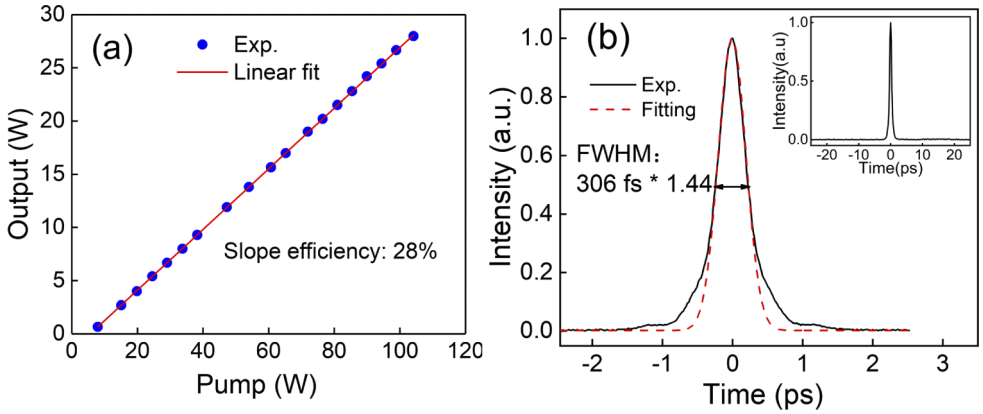

Fig. 4. Forward pumped amplifier results: (a) Amplified power (black dot) vs. incident pump power. (b) Autocorrelation trace for the pulse after compression at maximum compressed average power of 20 W. Inset: 50 ps span.

Optics EXPRESS

The total B-integral was calculated to be 1.85π (made up of 0.2π, 0.2π and 1.45π from fiber stretcher, pre-amplifier and power amplifier, respectively). By appropriate adjustment of the compressor grating separation, 306 fs duration pulses were obtained at the maximum compressed output power of 20 W (71.5% compressor transmission efficiency). The autocorrelation of the 1.27 μJ compressed pulses is shown in Fig. 4(b). The time bandwidth product (TBP) was calculated to be 0.99, which is 2.3 times the transform-limited value for a Gaussian pulse (0.44), but close to that of a transform-limited pulse with a rectangular-spectrum (0.88). It is worth noting that the TBP is nearly the same as when we recompressed the pulses emerging directly from the seed laser, indicating both the excellent dispersion balance between the stretcher and compressor and the minimal impact from nonlinearity in the amplifier. Based on the autocorrelation data, we calculate that 82% of the pulse energy resides in the main peak, implying a pulse energy of 1.04 μJ and a peak power of 3.4 MW at the centre of the pulse.

We next investigated backward pumping which reduces the effective nonlinear length. A mode field adapter (MFA) (AFR) at the amplifier input replaced the combiner. Free-space coupled end pumping via a dichroic mirror (high transmission at 793 nm, high reflectivity at 1925 nm) was used. Figure 5(a) shows the spectral output from the oscillator, pre-amplifier and main amplifier. An output power of 30 W (shown in Fig. 5(b)) was achieved at the maximum pump power of 100 W, at a slope efficiency of 32% with respect to the incident pump power. This was somewhat higher than the 28% achieved with forward pumping because the gain peak was shifted to shorter wavelengths with backward pumping. The measured fiber output had M_x^2 and M_y^2 of 1.09 and 1.12. In addition, the spatial mode out of the compressor was measured to have M_x^2 and M_y^2 of 1.10 and 1.12, respectively. which indicates close to a pure-single-mode was achieved from the system.

The pedestal on the AC due to nonlinear distortions when running at the maximum power is less pronounced with backward pumping (comparing Fig. 5(c) with Fig. 4(b)) and 91% of the energy remained in the main peak even though the power actually increased compared to forward pumping. The 21.5 W compressor output resulted in a corresponding pulse energy of 1.25 μJ and a peak power of 4.2 MW in the main peak, with a pulse duration of 297 fs, as shown in Fig. 5(c). The TBP of 0.96 is similar to the forward pumped result. The total B-integral of the system was calculated to have reduced to 1.15π (0.75π from the power amplifier). OH absorption peaks are clearly observable in the spectra shown in Fig. 3 and Fig. 5. These originate from free space propagation in air within the compressor (2.5 m total path length), and indeed within the OSA itself. However, autocorrelation trace data after the compressor indicates that the water absorption peaks do not severely affect the temporal pulse quality. Obviously these absorption peaks could be avoided if desired by suitably controlling the gas environment in the compressor.

The maximum pulse energy in our system was limited by the available pump power not by nonlinear effects. In order to explore the nonlinearity threshold (i.e. maximum pulse energy before spectral distortions were observed). We therefore inserted a pulse picker followed by an extra pre-amplifier stage before the power amplifier to scale the peak power. The nonlinear peak power threshold of the power amplifier, estimated the appearance of spectral wings (shown in the inset to Fig. 5(d)) on the pulses emerging directly from the fiber was 21 kW in the forward pumping embodiment and increased to 43 kW in the backward pumping scheme. This indicates that the theoretical maximum output peak-power of the compressed pulses from our system would be increased by a factor of ~2 to reach at 8.4 MW peak power after the compressor when using the backward pumping scheme. Further peak-power scaling beyond 10 MW would be enabled by employing a larger stretcher element in order to reduce the nonlinearity in the amplifiers at any given pulse energy. For example, this could be achieved with a longer stretcher fiber length; or using a double pass of the existing stretcher fiber; or by switching to a dispersion-tailored CFBG, and the new stretcher could be matched by e.g. a larger transverse dimension transmission grating

Optics EXPRESS

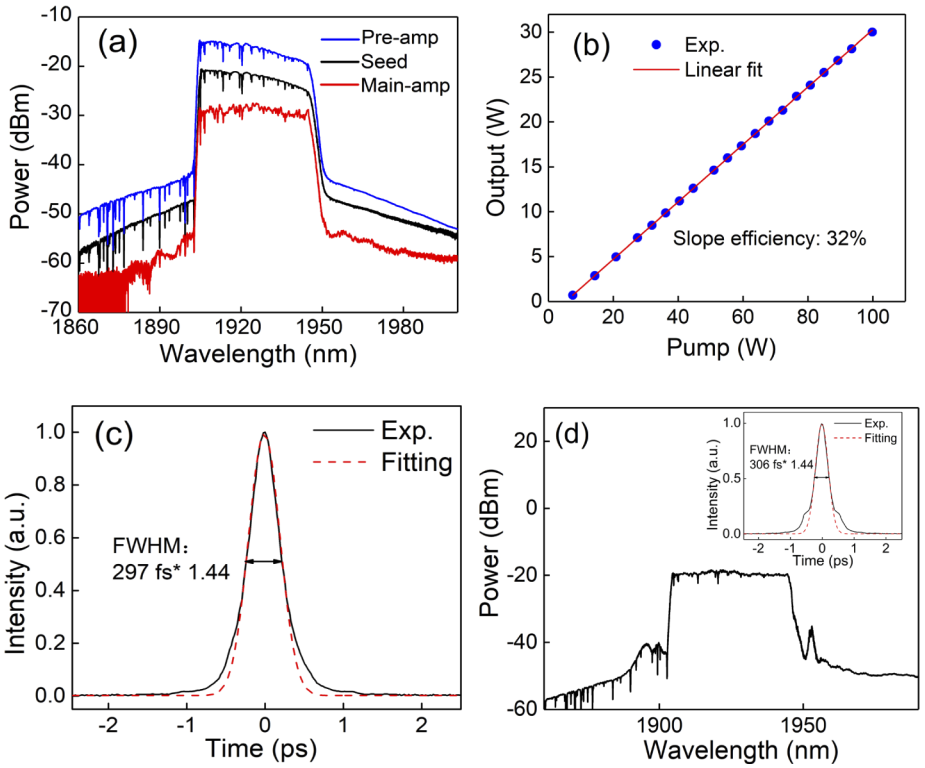

Fig. 5. Reverse pumping results. (a) Optical spectra after the oscillator (black), pre-amplifier (blue) and final amplifier amplified pulses (red) at the maximum output power using backward pumping. (b) Power (black dot) from final amplifier vs. incident pump power. (c) Autocorrelation trace at maximum compressed average power of 21.5 W. (d) Optical spectrum with sidebands over nonlinear peak power threshold; inset shows corresponding compression pulse autocorrelation trace.

pair or a CVBG compressor (Extending to those additional components was beyond our currently available resources).

4. Conclusion

In summary, we have experimentally demonstrated a compact, dissipative soliton seeded CPA system at 1925nm producing ~300 fs pulses at 15.7 MHz repetition rate and 21.5 W of output power from a fully fiberized seed laser and amplifier block. We avoided gain-narrowing by using the polarization controllers in the seed laser to pre-shape the spectrum at the amplifier input in order to obtain a flat spectrum after the impact of gain tilt in the main amplifier.

The chirped 25 ps pulses from the seed laser help to reduce the nonlinear phase accumulation in the fiber-based stretcher. After amplification of the pulses with the reverse pumped final amplifier configuration the pulses were re-compressed to a duration of 297 fs with 1.25 μJ of pulse energy and 4.2 MW peak power, which we found was a significant increase in energy to the maximum obtainable when using the forward pumped final amplifier configuration. In addition, backward pumping improve the compressed pulse quality, increasing the fraction of the energy in the main peak from 82% to 91%. Tests at lower repetition rates showed that significant further pulse energy scaling would be possible before nonlinear effects strongly distort the pulses. Hence by

Optics EXPRESS

operating at the full repetition rate of the laser and by using higher pump power in the backward pumped main amplifier, rather than the 100 W maximum available here, ought to provide >8 MW peak power and 40 W average power with the existing stretcher and compressor, or >10 MW peak power by increasing the stretching/compression ratio with more costly components.

Funding

Engineering and Physical Sciences Research Council (EP/P012248/1, EP/P027644/1, EP/P030181/1); Air Force Office of Scientific Research (FA9550-14-1-0382).

Acknowledgments

The data from the figures can be found in https://doi.org/10.5258/SOTON/D1049. Zhengqi Ren thanks the China Scholarship Council for financial support of his PhD.

References

1. R. G. Frehlich, S. M. Hannon, and S. W. Henderson, "Performance of a 2-μm coherent Doppler lidar for wind measurements," J. Atmos. Oceanic Technol. **11**(6), 1517–1528 (1994).
2. W. Shi, E. Petersen, N. Moor, A. Chavez-Pirson, and N. Peyghambarian, "All fiber-based single-frequency Q-switched laser pulses at 2 μm for lidar and remote sensing applications," Proc. SPIE **8164**, 81640M (2011).
3. V. Konov, "Laser in micro and nanoprocessing of diamond materials," Laser Photonics Rev. **6**(6), 739–766 (2012).
4. Q. Fu, L. Xu, S. Liang, D. P. Shepherd, D. J. Richardson, and S. Alam, "Widely Tunable, Narrow-Linewidth, High-Peak-Power, Picosecond Midinfrared Optical Parametric Amplifier," IEEE J. Quantum Electron. **24**(5), 1–6 (2018).
5. M. P. Arpin, T. Popmintchev, M. Gerrity, B. Zhang, M. Seaberg, D. Popmintchev, M. M. Murnane, and H. C. Kapteyn, "Bright, coherent, ultrafast soft X-ray harmonics spanning the water window from a tabletop light source," Phys. Rev. Lett. **105**(17), 173901 (2010).
6. E. A. Peralta, K. Soong, R. J. England, E. R. Colby, Z. Wu, B. Montazeri, C. McGuinness, J. McNeur, K. J. Leedle, D. Walz, E. B. Sozer, B. Cowan, B. Schwartz, G. Travish, and R. L. Byer, "Demonstration of electron acceleration in a laser-driven dielectric microstructure," Nature **503**(7474), 91–94 (2013).
7. F. Stutzki, C. Gaida, M. Gebhardt, F. Jansen, A. Wienke, U. Zeitner, F. Fuchs, C. Jauregui, D. Wandt, D. Kracht, J. Limpert, and A. Tünnermann, "152 W average power Tm-doped fiber CPA system," Opt. Lett. **39**(16), 4671–4674 (2014).
8. A. Klenke, S. Breitkopf, M. Kienel, T. Gottschall, T. Eidam, S. Hädrich, J. Rothhardt, J. Limpert, and A. Tünnermann, "530 W, 1.3 mJ, four-channel coherently combined femtosecond fiber chirped-pulse amplification system," Opt. Lett. **38**(13), 2283–2285 (2013).
9. A. Klenke, M. Müller, H. Stark, F. Stutzki, C. Hupel, T. Schreiber, A. Tünnermann, and J. Limpert, "Coherently combined 16-channel multicore fiber laser system," Opt. Lett. **43**(7), 1519–1522 (2018).
10. R. A. Sims, P. Kadwani, A. L. Shah, and M. Richardson, "1 μJ, sub-500 fs chirped pulse amplification in a Tm-doped fiber system," Opt. Lett. **38**(2), 121–123 (2013).
11. H. Hoogland and R. Holzwarth, "Compact polarization-maintaining 2.05-μm fiber laser at 1-MHz and 1-MW peak power," Opt. Lett. **40**(15), 3520–3523 (2015).
12. C. Gaida, M. Gebhardt, T. Heuermann, F. Stutzki, C. Jauregui, and J. Limpert, "Ultrafast thulium fiber laser system emitting more than 1 kW of average power," Opt. Lett. **43**(23), 5853–5856 (2018).
13. F. Tan, H. Shi, P. Wang, J. Liu, and P. Wang, "Chirped pulse amplification of a dissipative soliton thulium-doped fiber laser," Proc. SPIE **9728**, 97280Y (2016).
14. D. Gaponov, L. Lavoute, S. Février, A. Hideur, and N. Ducros, "2μm all-fiber dissipative soliton master oscillator power amplifier," Proc. SPIE **9728**, 972834 (2016).
15. P. Ciąćka, A. Rampur, A. Heidt, T. Feurer, and M. Klimczak, "Dispersion measurement of ultra-high numerical aperture fibers covering thulium, holmium, and erbium emission wavelengths," J. Opt. Soc. Am. B **35**(6), 1301–1307 (2018).
16. P. Elahi, H. Kalaycioğlu, Ö Akçaalan, Ç Şenel, and FÖ Ilday, "Burst-mode thulium all-fiber laser delivering femtosecond pulses at a 1 GHz intra-burst repetition rate," Opt. Lett. **42**(19), 3808–3811 (2017).
17. E. Desurvire, "Analysis of gain difference between forward- and backward-pumped erbium-doped fiber amplifiers in the saturation regime," IEEE Photonics Technol. Lett. **4**(7), 711–714 (1992).
18. S. Liang, L. Xu, Q. Fu, Y. Jung, D. P. Shepherd, D. J. Richardson, and S.-U. Alam, "295-kW peak power picosecond pulses from a thulium-doped-fiber MOPA and the generation of watt-level >2.5-octave supercontinuum extending up to 5 μm," Opt. Express **26**(6), 6490–6498 (2018).
19. G. J. Spühler, T. Südmeyer, R. Paschotta, M. Moser, K. J. Weingarten, and U. Keller, "Passively mode-locked high-power Nd:YAG lasers with multiple laser heads," Appl. Phys. B: Lasers Opt. **71**(1), 19–25 (2000).

Optics EXPRESS

20. C. Hönninger, R. Paschotta, F. Morier-Genoud, M. Moser, and U. Keller, "Q-switching stability limits of continuous-wave passive mode locking," J. Opt. Soc. Am. B **16**(1), 46–56 (1999).
21. A. Chong, J. Buckley, W. Renninger, and F. Wise, "All-normal-dispersion femtosecond fiber laser," Opt. Express **14**(21), 10095–10100 (2006).